jmr&t
Journal of Materials Research and Technology
www.jmrt.com.br

Original Article

Heat generation model for taper cylindrical pin profile in FSW

Vijay Shivaji Gadakh[a,b,*], Kumar Adepu[a]

[a] Department of Mechanical Engineering, National Institute of Technology, Warangal, India
[b] Department of Production Engineering, Amrutvahini College of Engineering, Sangamner, Ahmednagar, Maharashtra, India

ARTICLE INFO

Article history:
Received 16 March 2013
Accepted 10 October 2013
Available online 7 November 2013

Keywords:
Friction stir welding
Analytical modeling
Tool shape
Energy
Al alloys

ABSTRACT

Modeling offers great potential for reducing experimental effort in development of welding parameters, tool design and many other areas and at the same time reduce cost and time. An analytical model for heat generation for friction stir welding using taper cylindrical pin profile was developed. The proposed analytical expression is the modification of previous analytical models known from the literature which is verified and well matches with the model developed by previous researchers. The results of the proposed model were validated with the data from previous researchers. From the obtained results, it was observed that less temperature is generated using taper cylindrical pin profile than straight cylindrical pin profile under given set of working conditions. Furthermore, numerical simulation result shows that increasing the taper pin angle leads to decrease in peak temperature.

1. Introduction

Friction stir welding (FSW) [1–5] was invented at The Welding Institute (TWI) of UK in 1991 as a solid-state joining technique, and it was initially applied to aluminum (Al) alloys. Researchers all over the world now recognize the benefits of using solid-state welding process as potential measure for difficult-to-weld materials and for additive manufacturing. For example, friction stir processing (FSP) and friction welding, friction surfacing processes are under active consideration for additive manufacturing [6]. The science and technology is directed toward advanced equipment development, tool design and tool material development, welding process parameter optimization, understanding and predicting microstructural and mechanical property evolution during joining. By adapting the concepts of FSW, FSP have been developed for the fabrication of metal matrix composites (MMC) [7], surface modification [8]. During this process, the material undergoes intense plastic deformation at elevated temperature resulting in significant grain refinement. Tool geometry/design plays an important role in FSW/P process because it performs main functions such as (a) localized heating, (b) material flow and (c) stirring action. A number of researchers used different tool geometries/designs in order to improve the mechanical properties [9].

In the present work, an analytical model for heat generation for taper cylindrical (TC) pin profile in FSW was

* *Corresponding author.*
E-mail: gadakh_vijay@rediffmail.com (V.S. Gadakh).

2238-7854 http://dx.doi.org/10.1016/j.jmrt.2013.10.003

Nomenclature

Q_1	heat generation from shoulder surface
Q_2	heat generation from probe surface
Q_3	heat generation from tip surface
μ	friction coefficient
ω	tool angular rotation speed (rad/s)
α	tool pin taper angle (°)
v	tool speed of ωr (m/s)
σ	contact pressure (Pa)
$\tau_{Contact}$	contact shear stress (Pa)
R_{PT}	tool probe radius (mm) (taper)
R_{PS}	tool probe radius (mm) (straight)
$R_{Shoulder}$	tool shoulder radius (mm)
Q_{Total}	total heat generation (W)
H_{Probe}	tool probe height (mm)

developed. Nowadays, the analytical models developed are only for straight cylindrical pin (SC) pin profile. The need of developing analytical model is that for TC pin profile better mechanical properties were obtained than SC pin profile [10–14]. The proposed analytical expression is a modification of previous analytical models developed by Khandkar et al. [15] and Schmidt et al. [16]. Khandkar et al. [15] introduced a torque based heat input model for SC pin profile, where the torque/power known from experiments is used in the expression for the heat source. Furthermore, Schmidt et al. [16] developed an analytical model for heat generation for SC having concave shoulder in FSW based on different assumptions in terms of contact condition between the rotating tool surface and the weld piece. Biswas and Mandal [14] reported that tools having a concave shoulder led to lesser temperature rise. At the same time, conical tool pins exhibited somewhat lesser peak temperature compared to that of a SC pin profile. Gadakh and Kumar [17] have made an attempt to develop an analytical model for heat generation for TC pin profile but they have modeled it incorrectly.

From the experimental aspect various researchers reported better mechanical properties for TC pin profile. Suresha et al. [10] reveals that the conical tools show better joint efficiency compared to the square (SQ) tools. Hattingh et al. [11] found that taper pin angle is beneficial in producing the plastic flow conditions that are conducive to high strength welds. Buffa et al. [12] observed that increase in temperature is greater when the pin angle is small than that when pin angle is large. It is also important here to note that fine grain-sized product is always desired, so it is better to lower the working temperature where the grain growth during cooling from the working temperature is negligible called finishing temperature which is just above the minimum recrystallization temperature. In hot working processes grain size is favored by a low finishing temperature [18]. Mishra and Ma [9] reported that FSW/FSP parameters, tool geometry, composition of workpiece, temperature of the workpiece, vertical pressure, and active cooling exert significant influence on the size of the recrystallized grains in the FSW/FSP materials. As the pin taper angle increases, the contact area between the welding pin and workpiece increases which increases frictional heat, deformation energy and heat affected zone (HAZ). A SC pin profile is helpful for obtaining a smaller grain size, but the nugget area obtained by SC pin profile is smaller than that by TC pin profile. A bigger pin angle has a significant increase in nugget area, namely the core of the welding where the grain size is in the order of 2–5 μm, which eventually leads to enhanced nugget integrity. Lammlein et al. [13] stated that conical tool reduces the process forces drastically. The 90° tool welds retained a reasonable percentage of parent material strength (50–60%). The 90° tool was shown to work better than the 60°, 80°, or 120° tools. Small cone inclusive angles require higher spindle speeds and create more flash while large angles produce larger processed and HAZs.

Another motivation for development of the model is that Fujii et al. [19] reported that in case of 6061-T6, whose deformation resistance is relatively low, the tool shape does not significantly affect the microstructures and mechanical properties of the joints. They have reported that under almost all FSW conditions, defect-free FSW joints were obtained. Accordingly, the tensile strength is not affected by the tool shape. But from macrostructure, tunnel defects were seen for triangular (TRI) pin profile at 1500 rpm, 1000 mm/min. While Elangovan et al. [20] revealed that microstructure of FSP region produced by SQ pin profile at 1200 rpm contained fine equiaxed grains which is for superior tensile properties of the joints. Also, microhardness survey shows that greater hardness for the TC pin profile than the SC pin profile. Furthermore, from the macroscopic point of view, tunnel defects were seen for SC pin profile at 1400 and 1600 rpm; for TRI pin profile at 1600 rpm. The above two references appear to be conflicting with each other.

Kumar and Raju [21] have studied the influence of different tool pin profiles (TC, taper cylindrical with threaded (TCH), TRI, SQ, pentagon (PEN) and hexagon (HEX)) on microstructure and mechanical properties of FSWed copper and reported that joints made using SQ tool pin profile resulted in better mechanical properties compared to other tool pin profiles. Ramanjaneyulu et al. [22,23] studied the influence of different tool pin profiles such as TC; taper (TRI, SQ, PEN and HEX) on heat generation and microstructure of AA2014 aluminium alloy. They have reported that the rate of heat generation as well as peak temperatures are relatively higher in the case of non-circular pin profiles, increasing with the number of flats (i.e., SQ to HEX). From the reported literature, it is well understood that the pin geometry plays a vital role for material flow, temperature history, grain size and mechanical properties in FSW process. From these aspect, there is ardent need of a model for TC pin profile by which one can find the peak temperature at the weld zone so that severe softening in the HAZ because of reversion (dissolution) of Mg_2Si precipitates during weld thermal cycle can be minimised or avoided in case of Al–Mg–Si alloys [24] by controlling weld process parameters.

Modeling offers great prospects in the future for reducing experimental effort in development of welding parameters, tool design, machine design, clamping systems and many other areas, and with the large effort currently being made in modeling it is reasonable to expect a significant return on this investment [25]. The numerical method can solve complicated functions that are difficult to be solved by the analytical

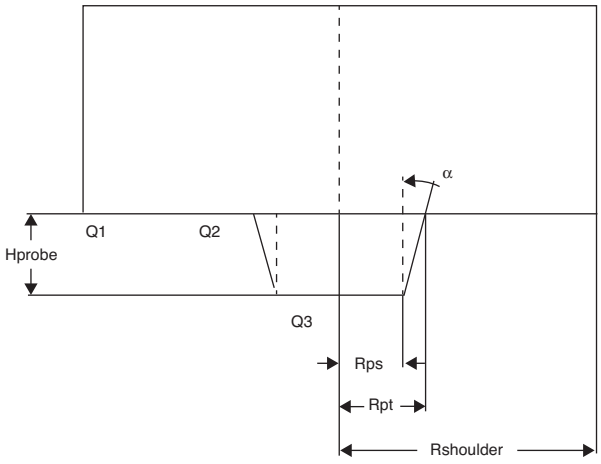

Fig. 1 – Different heat generation regions.

method. However, a numerical solution is discrete. On the other hand, the analytical method can solve relatively easy functions. Its solution is given by a formula that shows clearly the relationship between independent and dependent variables [26].

In this paper, combined approach of both methods was considered. In the first part an approximate analytical equation for heat generation was developed for TC pin profile and in the second part the effect of the taper pin on the temperature history was shown. The main objective was to estimate the heat generated due to plastic deformation and friction between the workpiece and tool surfaces. In order to verify the proposed model, this generated heat energy and the associated maximum temperature were compared to the results available in the literature.

2. Analytical estimation of heat generation

Fig. 1 shows three different regions where Q_1 is the heat generated under the tool shoulder, Q_2 at the tool pin side and Q_3 at the tool pin tip, hence the total heat generation, $Q_{total} = Q_1 + Q_2 + Q_3$.

The following underlying assumptions were made for the analytical modeling.

- The analytical estimation based on a general assumption of uniform contact shear stress $\tau_{contact}$ was considered.
- The sliding condition the shearing take place at the contact interface.
- Other mechanism of heat generation such as deformation was not considered.
- Due to friction interface conditions the frictional shear stress $\tau_{friction}$ was considered. The shear stress estimated for a sliding condition was $\tau_{contact} = \tau_{friction} = \mu p = \mu\sigma$

A simple tool design with flat shoulder surface, TC probe side surface and flat probe tip surface is assumed which is the modified version of the analytical model given by Schmidt et al. [16]. The TC pin surface is characterized by the taper angle α. The general equation for heat generation:

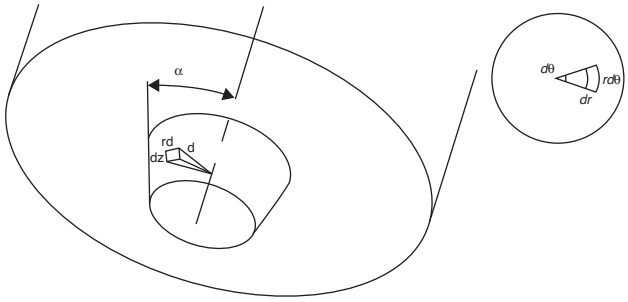

Fig. 2 – Surface orientations and infinitesimal segment areas for TC pin profile.

$$dQ = \omega \cdot dM = \omega \cdot r \cdot dF = \omega \cdot r \cdot \tau_{contact} \cdot dA \tag{1}$$

The contact surface between tool and workpiece given by position and orientation relative to rotation axis is shown in Fig. 2.

2.1. Heat generation from the shoulder surface

In order to calculate the heat generation in the shoulder surface rotating around the tool center axis, an infinitesimal segment on that surface is considered. The infinitesimal segment area $dA = r \cdot d\theta \cdot dr$ is exposed to a uniform contact shear stress $\tau_{contact}$. This segment contributes with an infinitesimal force of $dF = \tau_{contact} \cdot dA$ and torque of $dM = r \cdot dF$. The heat generation from this segment is

$$dQ = \omega \cdot r \cdot dF = \omega \cdot r^2 \cdot \tau_{contact} \cdot d\theta \cdot dr \tag{2}$$

where r is the distance from the considered area to the center of rotation, ω is the angular velocity, and $r \cdot d\theta$ and dr are the segment dimensions. Integration of Eq. (2) over the shoulder area from R_{PT} to $R_{shoulder}$ gives the shoulder heat generation, Q_1.

$$\begin{aligned} Q_1 &= \int_0^{2\pi} \int_{R_{PT}}^{R_{shoulder}} \omega \cdot r^2 \cdot \tau_{contact} \cdot d\theta \cdot dr \\ Q_1 &= \frac{2}{3}\pi\omega\tau_{contact}(R_{shoulder}^3 - R_{PT}^3) \end{aligned} \tag{3}$$

2.2. Heat generation from the taper probe surface

The probe consists of a taper cylindrical surface with a bottom radius of R_{PS}, top radius R_{PT} and probe height H_{probe}. The heat generated from the probe is given by Eq. (4) over the probe side area.

$$\begin{aligned} Q_2 &= \int_0^{2\pi} \int_0^{l} \omega \cdot r^2 \cdot \tau_{contact} \cdot d\theta \cdot dz \\ Q_2 &= 2 \cdot \pi \cdot \omega \cdot \tau_{contact} \cdot l \cdot \left(\frac{R_{PS} + R_{PT}}{2}\right)^2 \\ Q_2 &= \frac{\pi \cdot \omega \cdot \tau_{contact}}{2} \cdot \frac{H_{probe}}{\cos\alpha} \cdot (R_{PS} + R_{PT})^2 \end{aligned} \tag{4}$$

Table 1 – Material characteristics and tool geometry of the Al alloys [29].

Alloy	Thickness, t (mm)	$R_{Shoulder}$ (mm)	R_{PS} (mm)	H_{probe} (mm)	T_s (°C)
AA6061-T6	6.4	12	9.5	6	582
AA6061-T651	8.13	12.7	5	8	582
AA6082-T6	6	7.5	2.5	6	606
AA7050-T7451	6.4	10.2	3.6	6.1	488
AA7050-T7451	19.1	9.5	3.2	6.4	488

2.3. *Heat generation from the pin tip surface*

Integration of Eq. (2) over the pin tip surface, assuming a flat pin tip gives pin tip heat generation, Q_3.

$$Q_3 = \int_0^{2\pi}\int_0^{R_{PS}} \omega \cdot r^2 \cdot \tau_{contact} \cdot d\theta \cdot dr$$
$$Q_3 = \frac{2}{3}\pi \cdot \omega \cdot \tau_{contact} \cdot R_{PS}^3 \quad (5)$$

From Eqs. (3)–(5), Q_{Total} can be calculated as: $Q_{Total} = Q_1 + Q_2 + Q_3$

$$Q_{Total} = \frac{2}{3}\pi\omega\tau_{contact}(R_{shoulder}^3 - R_{PT}^3) + \frac{\pi \cdot \omega \cdot \tau_{contact}}{2} \cdot \frac{H_{probe}}{\cos\alpha} \cdot (R_{PS} + R_{PT})^2 + \frac{2}{3}\pi \cdot \omega \cdot \tau_{contact} \cdot R_{PS}^3$$

But,

$$R_{PS} = R_{PT} - H_{probe} \cdot \tan\alpha \quad (6)$$

Hence, Q_{Total} becomes,

$$Q_{Total} = \frac{2}{3}\pi\omega\tau_{contact} \cdot \left(R_{shoulder}^3 - R_{PT}^3 + \frac{3}{4} \cdot \frac{H_{probe}}{\cos\alpha} \cdot (2 \cdot R_{PT} - H_{probe} \cdot \tan\alpha)^2 + (R_{PT} - H_{probe} \cdot \tan\alpha)^3\right) \quad (7)$$

The energy per unit length of the weld can be calculated dividing Eq. (7) by the transverse speed:

$$Q_{Energy/length} = \frac{2}{3} \cdot \frac{\omega \cdot F \cdot \mu}{\nu \cdot R_{shoulder}^2} \cdot \left(R_{shoulder}^3 - R_{PT}^3 + \frac{3}{4} \cdot \frac{H_{probe}}{\cos\alpha} \cdot (2 \cdot R_{PT} - H_{probe} \cdot \tan\alpha)^2 + (R_{PT} - H_{probe} \cdot \tan\alpha)^3\right) \quad (8)$$

In the case of a SC pin profile, the heat generation expression simplifies to ($R_{PT} = R_{PS}$)

$$Q_{Total} = \frac{2}{3} \cdot \pi \cdot \omega \cdot \tau_{contact} \cdot (R_{shoulder}^3 + 3 \cdot H_{probe} \cdot R_{PS}^2) \quad (9)$$

This correlates with the results found by Khandkar et al. [15] or Schmidt et al. [16]. The same expression without the last term has been suggested by Frigaard et al. [27,28].

The energy per unit length of the weld can be calculated dividing Eq. (8) by transverse speed.

The shear stress estimates for a sliding condition is $\tau_{contact} = \tau_{friction} = \mu p = \mu\sigma$ and pressure equals to the force divided by the projected area.

$$Q_{Energy/length} = \frac{2}{3} \cdot \frac{\omega \cdot F \cdot \mu}{\nu \cdot R_{shoulder}^2} \cdot \left(R_{shoulder}^3 - R_{PT}^3 + \frac{3}{4} \cdot \frac{H_{probe}}{\cos\alpha} \cdot (2 \cdot R_{PT} - H_{probe} \cdot \tan\alpha)^2 + (R_{PT} - H_{probe} \cdot \tan\alpha)^3\right) \quad (10)$$

The effective energy per weld length (Q_{Eff}) [29] is defined as the energy per weld length multiplied by the transfer efficiency (β, ratio of the pin length H_{Probe} to the work piece thickness t) and given by:

$$Q_{Eff} = \frac{h}{t} \cdot Q_{Energy/length} = \beta \cdot Q_{Energy/length} \quad (11)$$

For validation of the proposed model, the empirical relationship developed by Hamilton et al. [29] between the temperature ratio and the effective energy level was considered. The empirical formula is given by

$$\frac{T_{max}}{T_s} = 1.56 \times 10^{-4} \times Q_{Eff} + 0.54 \quad (12)$$

The coefficient of friction (μ) varies with temperature. But in the present model for demonstration purpose it was considered as 0.5. Table 1 shows the material characteristics and tool geometry of the different Al alloys [29]. Table 2 shows welding process parameters $Q_{Energy/length}$ and T_{max} (°C) of the different Al alloys along with the results of this study considering zero taper angle α. Fig. 3 shows the variation of the peak temperature for the proposed model, Hamilton et al. [29] model, and Emam and Domiaty [30] results.

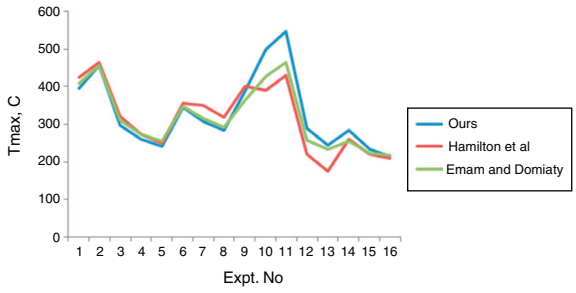

Fig. 3 – Variation of the peak temperature for the proposed model, Hamilton et al. [29] model and Emam and Domiaty [30] results.

Table 2 – Welding process parameters of the Al alloys and calculated peak temperature [30].

Alloy	rev min^{-1} (ω)	ν (mm min^{-1})	F (kN)	$Q_{Energy/length}$ (J mm^{-1}) [29]	$Q_{Energy/length}$ (J mm^{-1}) [30]	$Q_{Energy/length}$ (J mm^{-1}) ours	T_{max} (°C) [29]	T_{max} (°C) [30]	T_{max} (°C) ours
AA6061-T6	344	2.2	13	1639	1756	1652	425	408	395
AA6061-T651	390	2.4	22	1896	2049	2049	466	458	458
		5		696	791	696	321	310	297
AA6082-T6	1500	8	7	435	529	435	275	274	261
		12		290	384	290	250	254	241
		0.85	20	1845	1863	1845	355	349	347
	180	1.3	25	1513	1564	1508	350	315	309
		1.7	28	1273	1373	1291	320	293	284
AA7050-T7451	360	1.7	24	1978	1993	2214	400	363	388
	540	2.5	34	2464	2559	3199	390	428	500
	810	3.8	39	2868	2897	3621	430	466	548
	520	1	18	3053	3053	3816	220	259	290
		1.9	24	2410	2410	2678	175	234	244
AA7050-T7451		1	13	3710	2968	3710	260	256	286
	700	1.9	16	2403	2163	2403	220	224	234
		2.6	18	2229	1978	1976	210	217	217

3. Effect of taper angle on thermal history

In Fig. 4(a–c) under given set of conditions peak temperature goes on reducing. From Fig. 4(a) it is seen that for 59° taper angle temperature is 286 °C; beyond that R_{PT} becomes zero. For Fig. 4(b), 34° taper angle, temperature is 400 °C and for Fig. 4(c) 26° taper angle, it is 278 °C.

A similar trend is seen as suggested by Lammlein et al. [13]. They mentioned that 90° (here 45°) tool welds retained a reasonable percentage of parent material strength (50–60%) than the 60° (here 30°), 80° (here 40°), or 120° (here 60°) tools. Furthermore, Woo et al. [31] reported that in case of Al–Mg–Si alloys β'' precipitate phase begins at 216 °C and at 550 °C temperature there is complete dissolution of (β'') [32]. Considering the solvus temperature of the β'' (below 353 °C), the temperature inside the material during FSP can be high enough to dissolve the initial strengthening precipitates (β''), resulting in the microstructural softening for the precipitation-hardenable 6061-T6 Al alloys. Softening in the nugget zone and thermo-mechanically affected zone (TMAZ) is mainly related to the complete dissolution of needle-shape precipitates (β''), while the softening in the HAZ is due to the partial dissolution of (β'') and the growth of the rod-shape precipitates (β').

It is interesting to note that as taper pin angle increases (under constant shoulder to pin diameter ratio), the contact area of the probe with workpiece increases resulting in increase in friction and heat generation. Schmidt et al. [16] reported that maximum heat generated is due to tool shoulder (86%) than probe (11%) for SC pin profile which is approximately 8:1. This indicates that for SC pin profile due to small contact area of the probe with the workpiece, less heat is generated at the probe side. In short, the contact area of the probe with the workpiece in the case of SC pin profile is less as compared to the TC pin profile. So, the net heat flow is from probe toward the shoulder. However, the heat generated by the pin (%) is much lower [16]. As a consequence, the net result of temperature is always less than SC pin profile.

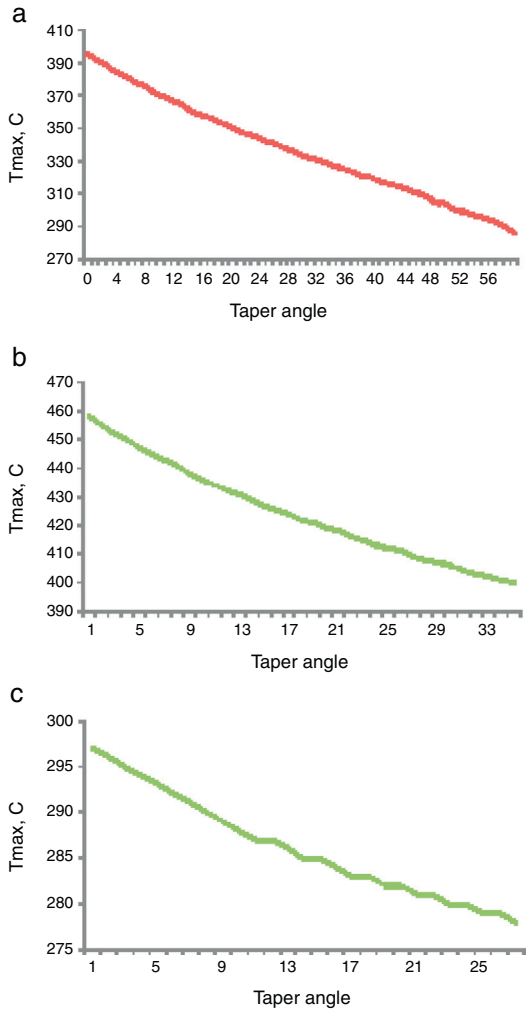

Fig. 4 – Effect of taper angle on peak temperature (a) AA6061-T6, (b) AA6061-T651 and (c) AA6082-T6.

Conflicts of Interest

The authors declare no conflicts of interest.

4. Conclusions

In this study, an analytical model for heat generation for FSW of Al alloy using taper cylindrical pin profile was developed. A combined of both analytical as well as numerical approach was considered. There is good agreement between the generated heat energy and the associated maximum temperature by the proposed model and results available in the literature. With the proposed analytical approach one can directly see the peak temperature for respective taper probe angle under given process conditions which will be helpful for predicting the mechanical properties for that Al alloy and hence elimination of post weld testing cost and time. The developed model described in this study with modification in Eqs. (11) and (12) can be used to predict the peak temperature for different alloys and materials.

REFERENCES

[1] Thomas WM, Nicholas ED, Needham JC, Murch MG, Templesmith P, Dawes CJ. Friction stir butt welding. US Patent 5,460,317; 1995.

[2] Dawes CJ, Thomas WM. Friction stir process welds aluminum alloys. Weld J 1996;75(3):41–5.

[3] Nicholas ED, Thomas WM. A review of friction processes for aerospace applications. Int J Mater Prod Technol 1998;13(1/2):45–55.

[4] Thomas WM, Threadgill PL, Nicholas ED. Feasibility of friction stir welding steel. Sci Technol Weld Join 1999;4(6):365–72.

[5] Thomas WM. Friction stir welding – recent developments. Mater Sci Forum 2003;426–432:229–36.

[6] Rao KP. Friction surfacing – a versatile technique. Prof. Dr. DRG Achar, memorial award for distinguished academician lecture. Southern zone: Indian Welding Society; 2011, January 22. p. 12.

[7] Bisadi H, Abasi A. Fabrication of Al7075/TiB_2 surface composite via friction stir processing. Am J Mater Sci 2011;1(2):67–70.

[8] Su JQ, Nelson TW, Sterling CJ. Friction stir processing of large-area bulk UFG aluminum alloys. Scripta Mater 2005;52:135–40.

[9] Mishra RS, Ma ZY. Friction stir welding and processing. Mater Sci Eng R 2005;50:1–78.

[10] Suresha CN, Rajaprakash BM, Upadhya S. A study of the effect of tool pin profiles on tensile strength of welded joints produced using friction stir welding process. Mater Manuf 2011;26(9):1111–6.

[11] Hattingh DG, Blignault C, Niekerk TIV, James MN. Characterization of the influences of FSW tool geometry on welding forces and weld tensile strength using an instrumented tool. J Mater Proc Technol 2008;203:46–7.

[12] Buffa G, Hua J, Shivpuri R, Fratini L. Design of the friction stir welding tool using the continuum based FEM model. Mater Sci Eng A 2006;419:381–8.

[13] Lammlein DH, DeLapp DR, Fleming PA, Strauss AM, Cook GE. The application of shoulderless conical tools in friction stir welding: an experimental and theoretical study. Mater Des 2009;30:4012–22.

[14] Biswas P, Mandal NR. Effect of tool geometries on thermal history of FSW of AA1100. Weld J 2011;90:129s–35s.

[15] Khandkar MZH, Khan JA, Reynolds AP. Prediction to temperature distribution and thermal history during friction stir welding: input torque based model. Sci Technol Weld J 2003;8:165–74.

[16] Schmidt H, Hattel J, Wert J. An analytical model for the heat generation in friction stir welding. Model Simul Mater Sci Eng 2004;12:143–57.

[17] Gadakh VS, Kumar A. Analytical model for heat generation for taper cylindrical pin profile for friction stir welding. In: Proc. of national welding seminar. 2013. Paper id-108 (CD-ROM).

[18] Dieter GE. Mechanical metallurgy. SI Metric Edition Singapore: Tata McGraw-Hill; 1988. p. 528–38.

[19] Fujii H, Cui L, Maeda M, Nogi K. Effect of tool shape on mechanical properties and microstructure of friction stir welded aluminium alloys. Mater Sci Eng A 2006;419: 25–31.

[20] Elangovan K, Balasubramanian V, Valliappan M. Effect of tool pin profile and tool rotational speed on mechanical properties of friction stir welded AA6061 aluminium alloy. Mater Manuf 2008;23(3):251–60.

[21] Kumar A, Raju LS. Influence of tool pin profiles on friction stir welding of copper. Mater Manuf 2012;27(12):1414–8, http://dx.doi.org/10.1080/10426914.2012.689455.

[22] Ramanjaneyulu K, Reddy GM, Rao AV, Markandeya R. Influence of tool pin profile on heat generation and microstructure of AA2014 aluminium alloy friction stir welds. In: Proc. of national welding seminar. 2013. Paper id-99 (CD-ROM).

[23] Ramanjaneyulu K, Reddy GM, Rao AV, Markandeya R. Structure–property correlation of AA2014 friction stir welds: role of tool pin profile. J Mater Eng Perform 2013, http://dx.doi.org/10.1007/s11665-013-0512-4.

[24] Reddy GM, Sammaiah P, Murthy CVS, Mohandas T. Influence of welding techniques on microstructure and mechanical properties of AA 6061 (Al–Mg–Si) gas tungsten arc welds. In: Proc. processing of metals. 2002. p. 33–46.

[25] Lohwasser D, Chen Z. Friction stir welding from basics to applications. UK: Woodhead Publishing Limited; 2009.

[26] Zhang XX, Xiao BL, Ma ZY. A transient thermal model for friction stir weld. Part II: Effects of weld conditions. Metall Mater Trans A 2011;42A:3229–39.

[27] Frigaard Ø, Grong Ø, Midling OT. A process model for friction stir welding of age hardening aluminium alloys. Metall Mater Trans A 2001;32:1189–90.

[28] Frigaard Ø, Grong Ø, Bjørneklett B, Midling OT. Modeling of the thermal and microstructural fields during friction stir welding of aluminium alloy. In: 1st int. symp. on friction stir welding. 1999.

[29] Hamilton C, Dymek S, Sommers A. A thermal model of friction stir welding in aluminum alloys. Int J Mach Tools Manuf 2008;48:1120–30.

[30] Emam SA, Domiaty AE. A refined energy-based model for friction-stir welding. WASET 2009;53:1016–22.

[31] Woo W, Choo H, Brown DW, Feng Z. Influence of the tool pin and shoulder on microstructure and natural aging kinetics in a friction-stir-processed 6061-T6 aluminium alloy. Metall Mater Trans A 2007;38A:69–76.

[32] Grong Ø, Bhadeshia HKDH, editors. Metallurgical modelling of welding. Materials modelling series. 2nd ed. London: The Institute of Materials; 1997.